Published on 20 February 2014. Downloaded by INDIAN INSTITUTE OF TECHNOLOGY BOMBAY on 10/20/2020 12:24:49 PM.

PCCP

PAPER

View Article Online
View Journal | View Issue

Magnetic exchange in {Gd^{III}–radical} complexes: method assessment, mechanism of coupling and magneto-structural correlations†

Cite this: *Phys. Chem. Chem. Phys.*, 2014, **16**, 14568

Tulika Gupta, Thayalan Rajeshkumar and Gopalan Rajaraman*

Received 15th January 2014,
Accepted 20th February 2014

DOI: 10.1039/c4cp00214h

www.rsc.org/pccp

Density functional studies have been performed on ten different {Gd^{III}–radical} complexes exhibiting both ferro and antiferromagnetic exchange interaction with an aim to assess a suitable exchange–correlation functional within DFT formalism. This study has also been extended to probe the mechanism of magnetic coupling and to develop suitable magneto-structural correlations for this pair. Our method assessments reveal the following order of increasing accuracy for the evaluation of J values compared to experimental coupling constants: B(40HF)LYP < BHandHLYP < TPSSH < PW91 < PBE < BP86 < OLYP < BLYP < PBE0 < X3LYP < B3LYP < B2PLYP. Grimme's double-hybrid functional is found to be superior compared to other functionals tested and this is followed very closely by the conventional hybrid B3LYP functional. At the basis set front, our calculations reveal that the incorporation of relativistic effect is important in these calculations and the relativistically corrected effective core potential (ECP) basis set is found to yield better Js compared to other methods. The supposedly empty 5d/6s/6p orbitals of Gd^{III} are found to play an important role in the mechanism of magnetic coupling and different contributions to the exchange terms are probed using Molecular Orbital (MO) and Natural Bond Orbital (NBO) analysis. Magneto-structural correlations for Gd–O distances, Gd–O–N angles and Gd–O–N–C dihedral angles are developed where the bond angles as well as dihedral angle parameters are found to dictate the sign and strength of the magnetic coupling in this series.

1 Introduction

Single molecule magnets (SMMs) have continued to be of interest to co-ordination chemists for the last two decades since the discovery of the {Mn12} cluster.[1,2] These types of molecules have a wide range of potential applications including miniaturisation of electronic devices, information storage devices, molecular spintronics, Q-bits in quantum computing and also has connection to nanotechnology and related applications.[1–4] Significantly, careful selection of inner magnetic core and outer ligand surroundings cause an inherent molecular spin inversion barrier (U_{eff}), high spin ground state, easy-axis magnetic anisotropy and blocking temperature (T_B) in SMMs.[1,5] These properties have triggered ground-breaking advances in this field over the last decade.[6]

Initial research efforts were focussed mainly towards the study of polynuclear 3d metal aggregates and manganese polynuclear complexes, which tend to increase the total spin (S) of the complexes (as high as 81/2 is achieved to-date[7]) but its counterpart, anisotropy (D), is found to decrease equally, leading to a decrease in the U_{eff} values.[8] Since controlling anisotropy becomes the most challenging task, new avenues such as lanthanide based molecular magnets are explored as these types of complexes possess significant magnetic anisotropy arising from the large unquenched orbital angular momentum. This leads to a steady increase in the number of SMMs based on lanthanide ions.[8,9] Despite the tremendous success with lanthanide ions in enhancing the U_{eff} values in short period of time, the T_B remains small due to very fast quantum tunnelling of magnetization (QTM).[10] Efforts to quench or decrease the QTM effects were undertaken and incorporation of 3d or radical centres along with the 4f ions, leading to a strong exchange interaction, is found to quench the QTM behaviour to a certain extent.[11] Of particular note here is the N_2^{3-} radical bridged {Ln_2} complexes, where strong exchange interaction is found between the radical and the lanthanide ions and this tends to increase the blocking temperature significantly. A preview of the literature immediately suggests that generally the exchange interactions in {4f–radical(2p)} combinations are stronger than {3d–4f} or {4f–4f} complexes. The {4f–2p} pair is also proposed to have many potential applications[12] on its own and exhibit versatile magnetic

Department of Chemistry, Indian Institute of Technology-Bombay, Powai, Mumbai, India. E-mail: rajaraman@chem.iitb.ac.in; Fax: +91-22-2572-3480; Tel: +91-22-2576-7183

† Electronic supplementary information (ESI) available. See DOI: 10.1039/c4cp00214h

This journal is © the Owner Societies 2014

Published on 20 February 2014. Downloaded by INDIAN INSTITUTE OF TECHNOLOGY BOMBAY on 10/20/2020 12:24:49 PM.

Table 1 The {Gd^{III}–radical} complexes reported in the literature with selected structural parameters and reported J values

Complexes	CSD ref code	J (cm^{-1})	Gd–O (Å)	Gd–O–N (°)	Gd–O–N–C (°)	Ref.
[Gd(NITtrz)$_2$(NO$_3$)$_3$]	—	6.10	—	—		19
[Gd(hfac)$_3$(NITPh-3-Br-4-OMe)$_2$] (**1**)	SICXEJ	5.69	2.312	139.95	80.01	20
[Gd(hfac)$_3$(NIT-5-Br-3py)]$_2$ (**2**)	NOMTIT	2.60	2.338	131.92	85.70	21
[Gd(hfac)$_3$(NITPh^{i}Pr)$_2$]	GIFNAM	2.42	2.346	139.67	87.90	11*g*
[Gd(hfac)$_3$(EtVNIT)$_2$] (**3**)	TEHZAJ	2.33	2.354	133.44	91.20	22
[Gd(hfac)$_3$(NITBzImH)]	WUPNIE	1.70	2.342	130.30	38.29	23
[Gd(hfac)$_3$(NIToPy)]	JOVZUP	1.52	2.322	124.30	50.07	24
[Gd(hfac)$_3$(NITPhOMe)$_2$]	MEMSUT	1.48	2.348	140.72	83.32	25
[Gd(hfac)$_3$(NITPhOMe)$_3$]$_2$ (**4**)	IPIDIV	1.46	2.358	135.86	91.96	26
[Gd(hfac)$_3$(NITpPy)]	JOWBAY	0.89	2.383	138.00	82.65	24
[Gd(hfac)$_3$(NITPhOCH$_2$Ph)$_2$]	KUPKIQ	0.62	2.342	138.15	81.41	27
[Gd(hfac)$_3$(NITPh-*p*-Cl)$_2$]	NIVQEO	0.62	2.354	143.20	89.95	28
[Gd(hfac)$_3$(NITPh)$_2$] (**5**)	FONMEA	0.61	2.327	141.10	92.37	29
[Gd(hfac)$_3$(NIT^{i}Pr)(H$_2$O)]	JEYJUS	0.21	2.410	147.00	95.72	30
[Gd(hfac)$_3$(NITPhOEt)$_2$] (**6**)	KUPKEM	0.27	2.316	137.19	84.72	27
[Gd(hfac)$_3$(NITEt)$_2$]	SAJBEK	0.25	2.337	144.60	95.13	31
[Gd(hfac)$_3$(NITPhOC$_4$H$_9$)$_2$]	ZAYKOB	0.10	2.331	139.07	84.85	32
[Gd(hfac)$_3$(NITPh-Ph)$_2$]	XIBTAF	0.05	2.350	136.51	79.37	33
[Gd(NITBzImH)$_2$(NO$_3$)$_3$]	PUZHON01	−0.80	2.365	136.38	32.96	19
[Gd(NITBzImH)$_4$](ClO$_4$)$_3$ (**7**)	LODJET01	−1.80	2.352	140.52	12.80	19
[Gd(hfac)$_3$(IMPy)]	XIVFOX01	−1.90	2.558[a]	116.67[b]	16.39[f]	23
[Gd(hfac)$_3$(IM$_2$imH)]	—	−2.59	—	—	—	34
[Gd(hfac)$_3$(IMBzIMH)]	WUPNOK	−2.60	2.599[a]	115.00[b]	5.59[f]	23
[Gd(hfac)$_3$(IM-2py)] (**8**)	XIVFOX	−3	2.540[a]	127.29[b]	15.40[f]	35
Gd(NITBzImH)$_2$(NO$_3$)$_3$	PUZHON01	−4.05	2.405	132.36	39.10	19
[Gd(hfac)$_3${2Py-NO}] (**9**)	FINHUH	−4.80	2.464	124.47	19.52	36
[Gd(Hbpz3)$_2$(dtbsq)] (**10**)	DIQROK	−5.7	2.349	119.14[c]	4.23[e]	14
[{[(Me$_3$Si)$_2$N]$_2$Gd(THF)}$_2$ (μ-η2:η2-N$_2$)]$^-$	UTESUI	−27	2.249[a]	143.52[d]	—	37
[Gd(hfac)$_3$(NIT-3BrPhOMe)]$_n$	—	—	2.385	145.40	91.30	38
[Gd(hfac)$_3$(ι-TTF + COO)]$_2$	—	—	2.379–2.381	—	—	39

[a] Gd–N distance. [b] Gd–N–C angle. [c] Gd–O–C angle. [d] Gd–N–Gd angle. [e] Gd–O–C–C dihedral angle. [f] Gd–N–C–C dihedral angle.

properties.[13] Organic radicals are of obvious choice because of its stability, ease of coordination to rare earths, direct bonding ability, synthetic accessibility and magnetic interaction ability to combine with rare earth ions. The {4f–2p} systems are found to exhibit the exchange coupling parameter ranging from moderate ferromagnetic to strong antiferromagnetic interaction (see Table 1).

In spite of numerous experimental studies on these {4f–2p} systems over the years, theoretical studies are still scarce.[14] Theoretical studies have played an indispensable role in the development of molecular magnets based on transition metal complexes,[15] and {3d–4f},[10a] and {4f–4f}[10b] complexes. Although thorough method assessment for transition metals,[16] {3d–4f}[17] and {4f–4f}[18] have been undertaken, a reliable methodology to compute magnetic exchange for the {Gd–2p} pair has not been established. Although the lack of anisotropy in Gd^{III} precludes SMM behaviour, its isotropicity results in a straightforward analysis of the magnetic exchange compared to its other lanthanide analogues and understanding of the magnetic coupling for this pair will help to design better SMMs with other anisotropic ions such as Dy^{III}.[11f] Here we aim to achieve the following: (i) perform method assessment with a range of exchange correlation functionals including pure, hybrid, meta-GGA and double-hybrid functionals; (ii) establish the general mechanism of magnetic coupling for {Gd–2p} pair; and (iii) develop magneto-structural correlation for this pair to ascertain the most influential structural parameter which affects the sign and strength of the J values.

2 Computational details

Absence of orbital contribution of the Gd^{III} ions allow the straightforward determination of the isotropic exchange coupling constant *via* isotropic Heisenberg–Dirac–Van Vleck (HDVV) spin Hamiltonian, which helps us to determine the magnetic exchange interaction between Gd^{III} and NITR radical in dinuclear complexes using the following spin-Hamiltonian:

$$H = -2JS_{Gd}S_{Rad}$$

Here S_{Gd} and S_{Rad} are spins on Gd^{III} (S = 7/2) and radical (S = 1/2) atoms, respectively. Where J is the isotropic exchange coupling constant, positive J values correspond to ferromagnetic coupling with high spin ground state (S = 4) and negative J values correspond to antiferromagnetic coupling with an S = 5/2 ground state. The DFT calculations combined with the broken symmetry (BS) approach[40] has been employed to compute the J values.[41] This methodology has a proven record of yielding good numerical estimate of J constants for a variety of complexes.[16,42]

The energy of the high spin state can be computed easily using a single determinant wave function such as a DFT method. However for the low spin state some approximations are required due to its multi-determinantal characteristics. The broken symmetry model developed by Noodleman[40] has been widely used in this regard.[16,42,43] This provides a good approximation of the energy of the low spin state and one can compute J values using HF or DFT calculations. Here all the calculations were performed using the

Published on 20 February 2014. Downloaded by INDIAN INSTITUTE OF TECHNOLOGY BOMBAY on 10/20/2020 12:24:49 PM.

Gaussian09[44] suite unless otherwise mentioned. As earlier method assessment for the {3d–4f} and {Gd–Gd} pair suggests that functionals play a critical role in the estimate of the exchange interaction, we have carried out a limited assessment for the basis set.[17,18] Unless otherwise mentioned all the calculations are performed using a double-zeta quality basis set employing Cundari–Stevens (CS) relativistic effective core potential (ECP) on Gd atoms[45] and the triple zeta basis set proposed by Schafer *et al.*[46] for the rest of the elements. Besides, we have also tested some all electron basis sets {Segmented All electron Relativistically contracted (SARC[47])} including the relativistic corrections using zeroth order regular approximation (ZORA[48]) or the Douglas–Kroll–Hess (DKH[49]) method. These basis tests were performed using the B3LYP functional and ORCA software suite.[50]

3 Results and discussion

There are numerous {Gd–2p} radical complexes reported in the literature and the reported complexes are listed in Table 1 with the estimated experimental J values. In these {Gd–2p} pairs, the Gd–O/N distances, Gd–O–N angles and Gd–O–N–C are the key parameters that are likely to influence the magnitude of the J values and these parameters for all thirty structures are also listed in Table 1. Out of these reported complexes, we have chosen ten different complexes where J values vary from strong ferromagnetic exchange to strong antiferromagnetic exchange. Thus our test set includes six ferromagnetic complexes (complexes **1** to **6** in Tables 2 and 4) and four antiferromagnetic complexes (complexes **7** to **10** in Tables 3 and 5) where the J is found to vary between -1.8 cm^{-1} to +5.9 cm^{-1}.

Description of the chosen models

The complexes **1–10** are chosen to understand the variation in the nature of exchange covering the range from strong ferromagnetic to strong antiferromagnetic interaction. In order to fulfil this purpose, we have selected diverse structures possessing both oxygen and nitrogen based radical systems. In the chosen set diverse radical ligands are co-ordinated, including nitronyl nitroxide with different substituents (bromine, methoxy, pyridine, ethoxy, benzoimidazole, (**1–7**)), imino nitroxide radical containing pyridyl unit (**8**), 2-pyridyl nitroxide (**9**) and semiquinonato radical ligands (**10**). A closer look at the Table 1 reveals that nitronyl nitroxide radicals always yield ferromagnetic interaction except in one case (complex **7**), whereas other radical ligands always yield antiferromagnetic coupling. For complexes **1–7** {Gd–radical}, one dimensional chains are reported and these are modelled as {Gd–radical} dimers to probe particularly the {Gd–radical} interaction.[46–48,52,53,55,58] The structure of the complexes studied here is shown in Fig. 1. In all the complexes **1–10**, the Gd^{III} ion is eight co-ordinated and this has been maintained in modelling the {Gd–radical} pairs.

Complexes **1–7** possess nitronyl nitroxide radicals with versatile substitution at the central C position. The Gd–O distances are found to vary in the range of 2.312 to 2.358 Å, the Gd–O–N angles are in the range of 131.9° to 141.1° and the Gd–O–N–C dihedral angles range from 12.80° to 95.72°. In complex **8**, the imino nitroxide radical containing a pyridyl unit is attached to Gd^{III} with one N of the imidazole ring connected to O (*i.e.* to form nitroxide). Here the nitrogen atoms are found to coordinate to the Gd^{III} ions, unlike in structures **1–7** where the oxygen atom was found to coordinate to the metal ion. The Gd–N distance is found to be 2.54 Å and this is much longer than the Gd–O distances found for structures **1–7**. In complex **8**, the radical NO centre is not directly coordinated to the Gd^{III} ion and thus this structure is peculiar as the magnetic exchange propagated here is super-exchange in nature while in all other cases, a direct exchange is expected. In complex **9**, a nitroxide radical is bridged to Gd^{III} while in complex **10** a

Table 2 Computed J values for complexes **1–6** and the standard deviation (SD) and mean absolute error (MAE) values with respect to experimental values

	1		**2**		**3**		**4**		**5**		**6**				
Functionals	J (cm^{-1})	SD	J (cm^{-1})	SD	J (cm^{-1})	SD	J (cm^{-1})	SD	J (cm^{-1})	SD	J (cm^{-1})	SD	Basis set	Relativis.	MAE
Exp	5.69	0	2.60	0	2.33	0	1.46	0	0.61	0	0.27	0			
B3LYP	3.91	0.89	4.94	1.17	4.31	0.99	4.03	1.29	2.71	1.05	3.28	1.51	Gd(CSDZ) and others (TZV)	ECP	1.66
B3LYP	−6.47	3.23	−5.40	3.7	−6.96	3.48	−10.1	5.05	−6.33	3.17	−6.1	3.05	Gd(SARC) and others TZVP	No	8.22
B3LYP	0.26	0.13	0.91	0.46	1.52	0.76	1.17	0.59	−0.69	0.35	−0.12	0.06	Gd(SARC) and others TZVP	ZORA	3.25
B3LYP	0.16	0.08	0.80	0.40	1.32	0.66	1.04	0.52	−0.74	0.37	−0.13	0.07	Gd(SARC) and others TZVP	DKH	2.21

Table 3 Computed J values for complexes **7–10** and the SD and MAE values with respect to experimental values

	7		**8**		**9**		**10**				
Functionals	J (cm^{-1})	SD	J (cm^{-1})	SD	J (cm^{-1})	SD	J (cm^{-1})	SD	Basis set	Relativis.	MAE[a]
Exp	−1.8	0	−3	0	−4.796	0	−5.7	0			
B3LYP	−1.28	0.26	−2.32	0.34	−3.66	0.57	−6.2	0.25	Gd(CSDZ) and others (TZV)	ECP	1.66
B3LYP	−8.56	4.28	−3.36	1.68	−8.30	4.15	−22.91	11.46	Gd(SARC) and others TZVP	No	8.22
B3LYP	−3.08	1.54	−4.16	2.08	−8.42	4.21	−10.80	5.4	Gd(SARC) and others TZVP	ZORA	3.25
B3LYP	−3.60	1.8	−3.95	1.98	−8.02	4.01	−11.34	5.67	Gd(SARC) and others TZVP	DKH	2.21

[a] $\mathrm{MAE} = \frac{1}{n}\sum_{i=1}^{n}\left|J_i^{\mathrm{calc}} - J_i^{\mathrm{exp}}\right|$.

 This journal is © the Owner Societies 2014

Published on 20 February 2014. Downloaded by INDIAN INSTITUTE OF TECHNOLOGY BOMBAY on 10/20/2020 12:24:49 PM.

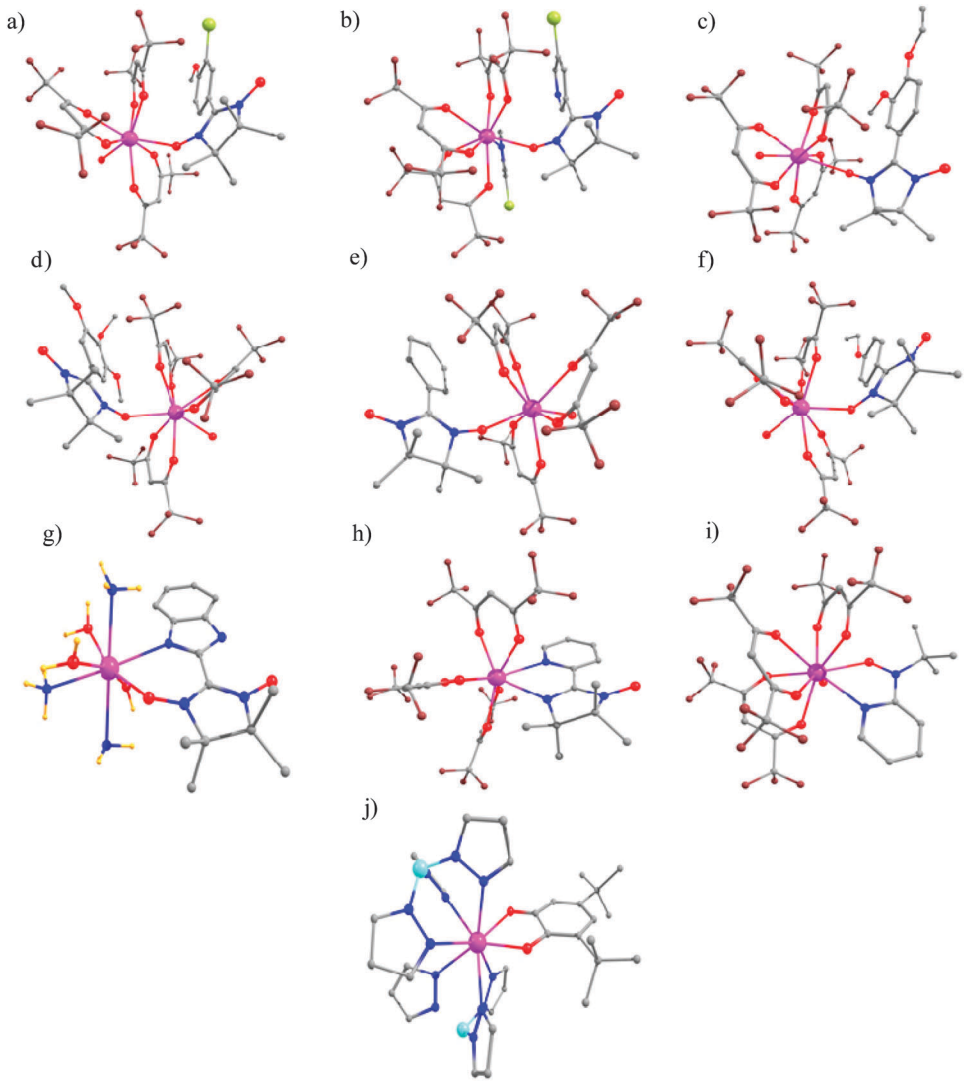

Fig. 1 X-ray structures of the complexes/models studied here (a) **1**, (b) **2**, (c) **3**, (d) **4**, (e) **5**, (f) **6**, (g) **7**, (h) **8**, (i) **9**, (j) **10**. (Colour scheme: Gd = pink, C = grey, O = red, N = blue, H = yellow, F = brown, Br = green.)

semiquinonato radical has bound to the Gd^{III} ion. The Gd–O distances here are similar to those found in complexes **1–7**.

Method assessment for the evaluation of magnetic exchange in {Gd^{III}–radical} systems

Effect of basis set on the estimation of exchange coupling constants. To test the effect of basis set on the estimation of *J* values, we have chosen all ten complexes described earlier and have selected four different set ups. The first set up comprises Cundari Stevens Double Zeta (CSDZ) ECP basis set for Gd^{III} and TZV for the rest of the elements (BS-I), the second set up comprises all electron SARC basis set for the Gd^{III} and TZVP for the rest of the elements (BS-II), the third set up comprises the same as BS-II but relativistic effects are incorporated using ZORA methodology (BS-III) while the fourth set up incorporates relativistic effects using DKH Hamiltonian on BS-II (BS-IV). The computed results are summarized in Tables 2 and 3. The BS-I set up yields accurate estimation of *J* values reproducing the sign correctly in all ten cases tested and also predicts the relative strength between the molecules correctly. The BS-II set up, which lacks relativistic effect, has not reproduced the sign correctly for all the ferromagnetic examples (**1–6**), while overestimating the antiferromagnetic *J*s (**6–10**). The BS-III set up improves the values obtained from BS-II and in many cases corrects the *J*s in the right direction, however still predicts wrong sign in two cases. The BS-IV set up is very similar to BS-III, and also predicts the wrong sign for two examples studied. This suggests that although Gd^{III} is isotropic, the relativistic effects are important and need to be incorporated in one way or another to obtain a reasonable estimate of magnetic coupling. Among all the set ups tested, the BS-I has the lowest mean absolute error (MAE) while BS-II yields the highest value. This suggests that incorporation of relativistic effect *via* CSDZ ECP is superior to ZORA/DKH methodology and this also has an advantage in terms of CPU timing, thus here onwards we continue to use the BS-I set up.

Published on 20 February 2014. Downloaded by INDIAN INSTITUTE OF TECHNOLOGY BOMBAY on 10/20/2020 12:24:49 PM.

Effect of exchange–correlation functionals on the estimation of exchange coupling constants. Although the $\{Gd_2N_2^{3-}\}$ radical system was studied by us earlier[51] using a hybrid functional (B3LYP), a rigorous method assessment with new generation functionals such as double-hybrids have not been attempted. Earlier studies on Gd^{III} based systems reveal that pure exchange–correlation functionals fail to predict the correct sign for {3d–4f}[17] and {Gd–Gd} dimers,[18] whereas the hybrid functionals generally yield good numerical estimate of the exchange interaction. To perform the method assessment on the chosen set of complexes, here we have chosen some GGA functionals (BP86,[52] PBE[53] BLYP,[52b,54] OLYP,[55] PW91[56]), some hybrid GGA functionals (PBE0,[53,57] B3LYP[52b,54,58]), a meta-hybrid GGA (TPPSH[57c,59]) and a double hybrid functional (B2PLYP[60]). In addition to this, we have also tested the B3LYP functional with 40% HF exchange (B(40HF)LYP) and half-and-half functional (BHandHLYP[54,58a,61]) possessing 50% HF exchange to probe the role of HF exchange in evaluating the *J* values. The computed *J* values are shown in Tables 4 and 5.

Performance of the different functionals against the experimental *J* values is depicted in Fig. 2 (see also Fig. S1 and S2 of ESI†). Computed standard deviation (SD) and the corresponding MAE[59] values are given in Tables 2–5. Our results reveal that except B(40HF)LYP and BHandHLYP functionals, all other functionals reproduce the sign of *J* values correctly in accordance with the experimental observation. The *J* values computed using all the functionals are above the experimental curve (see Fig. 2) with the exception of complexes **1** and **2**. This suggests that unilaterally all the functionals tend to overestimate the ferromagnetic part of the coupling for both the ferro and antiferro sets tested. All of the five tested pure functionals tend to move further away from the experimental curve compared to the other functionals. Among the tested pure functionals, BLYP and OLYP values are merely superimposable while the BP86, the PW91 and the PBE functionals offer distinctly different values. This suggests that the magnitude of exchange interaction is strongly correlated to the correlation part of the exchange–correlation functional. Among the tested pure functionals, the BLYP functional yields the lowest MAE for the entire test set.

The *J* values computed using TPSSH functional are much larger than the values computed using other functionals which leads to a large deviation in the computed parameters (SD and MAE). Among the hybrid functionals tested both B3LYP and X3LYP predict the same trend as both the functionals have the common LYP correlation, while the values computed using PBE0 functionals are slightly overestimated.[16,62] Among all the tested functionals Grimme's double hybrid B2PLYP offers very good estimate of the exchange (lowest MAE value of 1.35)

Table 4 Computed *J* values for complexes **1–6** and the SD and MAE values with respect to experimental *J* values

		1		**2**		**3**		**4**		**5**		**6**		
Functionals	% of HF exchange	J (cm^{-1})	SD	J (cm^{-1})	SD	J (cm^{-1})	SD	J (cm^{-1})	SD	J (cm^{-1})	SD	J (cm^{-1})	SD	MAE
Exp		5.69	0	2.60	0	2.33	0	1.46	0	0.61	0	0.27	0	
B3LYP	20	3.91	0.49	4.94	0.65	4.31	0.55	4.03	0.71	2.71	0.58	3.28	0.83	1.67
X3LYP	21.8	3.83	0.52	4.84	0.62	4.21	0.52	4.03	0.71	2.71	0.58	3.92	1.01	1.71
PW91	0	4.58	0.31	5.94	0.93	5.31	0.83	4.91	0.96	3.26	0.73	3.92	1.01	2.16
BHandHLYP	50	−1.67	2.04	−0.59	0.88	0.13	0.61	−0.39	0.51	2.30	0.47	−1.87	0.59	4.32
B(40HF)LYP	40	−5.41	2.67	−3.93	1.81	2.91	0.16	−3.20	1.29	5.81	1.44	−5.45	1.59	5.56
TPSSh	10	6.3	0.17	7.57	1.38	6.77	1.23	6.28	1.34	4.64	1.12	5.40	1.42	2.86
BP86	0	4.78	0.25	6.15	0.98	5.14	0.88	4.71	0.90	3.47	0.79	3.69	0.95	2.08
PBE	0	4.63	0.29	6.03	0.95	5.38	0.85	4.69	0.90	3.30	0.75	3.67	0.94	2.14
PBE0	25	4.48	0.34	5.52	0.95	4.83	0.69	4.52	0.85	3.11	0.69	3.76	0.97	1.82
B2PLYP	53	3.53	0.60	4.17	0.44	3.54	0.34	3.36	0.53	2.08	0.41	3.28	0.83	1.35
BLYP	0	3.78	0.53	5.06	0.68	4.49	0.60	4.15	0.75	2.64	0.56	3.20	0.81	1.85
OLYP	0	4.1	0.44	5.45	0.79	4.74	0.67	4.38	0.81	2.89	0.63	3.54	0.91	1.88

Table 5 Computed *J* values for complexes **7–10** and the SD and MAE values with respect to experimental values

		7		**8**		**9**		**10**		
Functionals	HF exchange (%)	J (cm^{-1})	SD	J (cm^{-1})	SD	J (cm^{-1})	SD	J (cm^{-1})	SD	MAE
Exp		−1.8	0	−3.0	0	−4.80	0	−5.70	0	
B3LYP	20	−1.28	0.14	−2.26	0.21	−3.66	0.32	−6.18	0.13	1.67
X3LYP	21.8	−1.28	0.14	−2.32	0.19	−3.66	0.32	−6.20	0.14	1.71
PW91	0	−0.58	0.34	−2.06	0.26	−4.01	0.22	−7.20	0.42	2.16
BHandHLYP	50	−5.81	1.11	−4.87	0.52	−10.53	1.59	−18.9	3.66	4.32
B(40HF)LYP	40	−8.36	1.82	−7.07	1.13	−15.7	3.02	−29.3	6.55	5.56
TPSSh	10	0.22	0.56	−2.28	0.20	−3.25	0.43	−5.37	0.09	2.86
BP86	0	−0.18	0.45	−1.9	0.31	−3.75	0.29	−5.97	0.07	2.08
PBE	0	−0.55	0.35	−2.05	0.26	−4.03	0.21	−7.24	0.43	2.14
PBE0	25	−1.26	0.15	−2.41	0.16	−3.68	0.31	−6.01	0.09	1.82
B2PLYP	53	−2.21	0.11	−2.15	0.24	−4.60	0.06	−6.40	0.19	1.35
BLYP	0	−0.93	0.24	−2.03	0.27	−4.02	0.22	−7.36	0.46	1.85
OLYP	0	−1.42	0.10	−2.24	0.21	−4.28	0.14	−7.52	0.50	1.88

 This journal is © the Owner Societies 2014

Published on 20 February 2014. Downloaded by INDIAN INSTITUTE OF TECHNOLOGY BOMBAY on 10/20/2020 12:24:49 PM.

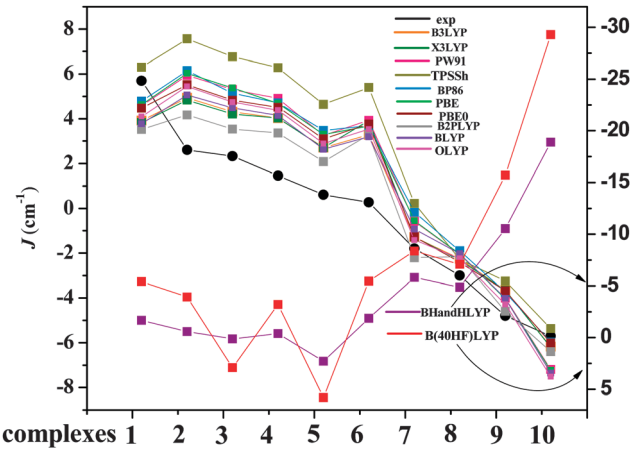

Fig. 2 Performance of different exchange–correlation functionals for the evaluation of J values. The experimental values for complexes **1–10** are given in black circles connected by the solid black line. Refer to right side y-axis for the B(40%HF)LYP and BHandHLYP functionals.

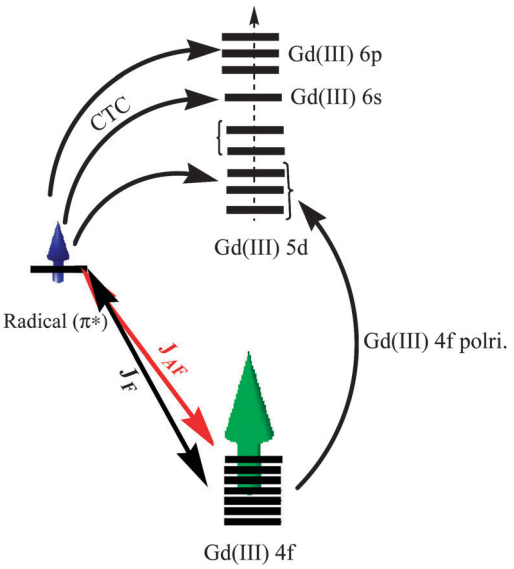

Scheme 1 Schematic illustration of the mechanism of magnetic coupling for a {Gd^{III}–radical} pair.

and is marginally better than the hybrid B3LYP functional (1.67). For most of the complexes the addition of perturbative correlation contribution corrects the J values in the right direction and is robust compared to standard MP2 calculations, which often fail miserably for such systems.[63] A similar conclusion has also been derived earlier.[64] The following order of increasing accuracy has been detected in this work for the estimation of magnetic exchange for the {Gd–radical} coupling B(40HF)LYP < BHandHLYP < TPSSH < PW91 < PBE < BP86 < OLYP < BLYP < PBE0 < X3LYP < B3LYP < B2PLYP.

The computed spin density values and the <S**2> values for complexes **1–10** with different functionals are listed in Table S3 of ESI.† The magnitude of spin density on the Gd^{III} ion is predicted to be larger than 7.0 by all functionals except BHandHLYP and B(40HF)LYP. Large spin density values on the radical centres were estimated by B2PLYP functional (in fact the largest among all the computed functionals) compared to B3LYP and this suggests that B2PLYP offers more localized description for the unpaired electron distribution and this in turn improves the estimate of J values (see ESI,† Fig. S3).

Mechanism of magnetic coupling in {Gd^{III}–radical} systems

To explore the mechanism that controls the nature of exchange, MO and NBO analysis have been performed in four complexes: **2**, **5**, **7** and **9**. Generally the net exchange parameter (J) originates from the contribution of antiferromagnetic (J_{AF}) and ferromagnetic (J_F) part of the exchange and some clues into these individual contributions can be gained by analysing the Molecular Orbitals and Natural Bonding Orbitals. The antiferromagnetic part of J (J_{AF}) is related to the overlap between the magnetic orbitals of the Gd^{III} and the π* orbitals of the radical centre. If the orbitals are orthogonal this would then contribute to J_F part. Besides the empty 5d/6s/6p orbitals, 4f of the Gd^{III} also participates in the mechanism of coupling as 4f orbitals are contracted and are generally inert in nature. Formally empty 5d/6s/6p orbitals of the Gd^{III} ions gain partial occupation from the radical centre *via* charge transfer mechanism and this type of acceptor–donor interaction contributes solely to ferromagnetic part of the exchange. Apart from the charge transfer there are also other ways by which the empty orbitals gain electrons.[65] The nature of the net exchange is usually decided by the dominant factor between the two terms. A generic mechanism of coupling incorporating all the above points is shown in Scheme 1 (see also Fig. S4 of ESI†).

In the case of complexes **2** and **5**, significant 4f–π* overlap is detected, with two significant interactions for complex **2** and three significant interactions for complex **5** (see ESI† Table S1 for computed overlap integral values, see also see Table S2 of the ESI†). This suggests a larger J_{AF} contribution for **5** compared to **2**. NBO second order perturbation analysis reveals a significant radical 2p to 4f donation, which contributes to the J_F part of the exchange. Some of the significant donor–acceptor interactions between the radical (2p) → Gd (5d/6s/6p) orbitals are shown in Fig. 4 (also see Fig. S4 of ESI†). The stabilization energies for these interactions are found to be 19.27, 14.71, 10.08, 6.53, 6.26 and 6.04 kcal mol^{-1} in the case of complex **5** and 12.41, 12.22, 11.46, 6.95, 5.38 and 5.07 kcal mol^{-1} for complex **2**. This reveals a larger J_F contribution for **5** compared to complex **2**. Thus our analysis suggests that complex **2** has a smaller J_{AF} contribution and larger J_F contribution compared to complex **5** and this leads to a larger positive value for **2** ($J_{exp.}$ 2.6 cm^{-1} *vs.* 0.6 cm^{-1} for **2** and **5**, respectively). The reason for these differences is likely to be attributed to the larger difference in the Gd–O–N angles between these two structures (131.9 *vs.* 141.1° for **2** and **5**, respectively).

Similarly for complexes **7** and **9**, three and five prominent 4f–π* overlaps are detected (see Table S3 and Fig. S4 and S6–S9 of ESI†). The J_F contribution is found to be larger for **7** compared to **9** as revealed by the NBO second-order PT energies (25.30, 19.86, 8.67, 6.17 and 6.08 kcal mol^{-1} for **7** and 24.41, 9.66 and 8.41 kcal mol^{-1} for **9**). Thus, here complex **9** has a

Published on 20 February 2014. Downloaded by INDIAN INSTITUTE OF TECHNOLOGY BOMBAY on 10/20/2020 12:24:49 PM.

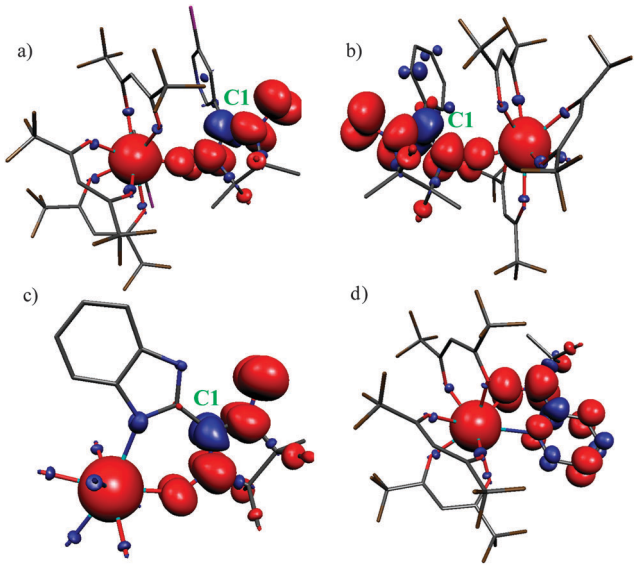

Fig. 3 Computed spin density plots for the HS state of complexes (a) **2**, (b) **5**, (c) **7** and (d) **9**.

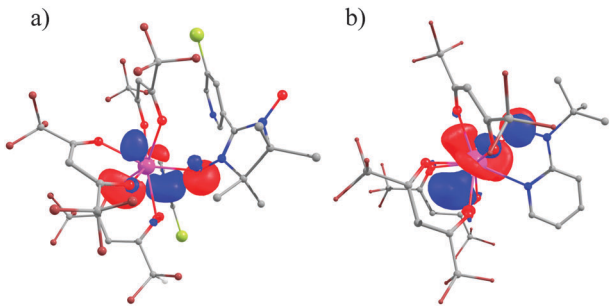

Fig. 4 Second order perturbation theory computed donor–acceptor NBO plot for the HS state in complex (a) **2** between Gd (p–d hybrid) and radical (s–p hybrid) orbital and (b) **9** between Gd (p–d hybrid) and radical (s–p hybrid) orbital.

larger J_{AF} contribution and a smaller J_F contribution compared to complex **7**, leading to larger AF coupling for complex **9** ($J_{exp.}$ -4.8 cm^{-1} *vs.* -1.8 cm^{-1} for **9** and **7**, respectively). As we go from **2** to **9**, the J_{AF} contribution increases as the number of overlap integral values increase. At the same time the magnitude and the number of J_F contribution also decreases. Thus, both these individual contributions readily explain the trend observed among these four complexes tested.

The spin density plots of the high-spin state for all four complexes are shown in Fig. 3 (for other complexes see ESI,† Fig. S5). The spin density of the Gd^{III} ion is found to vary from 7.03–7.04 with a spherical spin density shape. All the atoms coordinated to Gd^{III} are found to have negative spin densities except the radical ligand. This illustrates that the spin polarization mechanism is operational. The radical centres are not particularly localized to one atom but are completely delocalized across two NO moieties *via* spin polarization (note that the central C1 carbon has significant negative spin density, see Fig. 3) for the nitronyl nitroxide type radicals. For complex **9** both the coordinated O and the N atoms of the NO radical have equivalent distribution of spin density and the pyridyl ring also gains significant spin density from the radical centre (see Fig. 3d). The magnitude of spin density on the radical centres are diverse and are in the range of 0.16 to 0.44 for the O-atom coordinated to the Gd^{III} and as the spin density value increases, the antiferromagnetic part of the J is also found to increase.

Magneto-structural correlations

Magneto-structural correlations offer a way to relate the computed J values to a particular structural parameter and are very important in order to understand the trend observed among the given set of structures and also for future design of such complexes. In the set of complexes studied the Gd–O distance and Gd–O–N angles are likely to play a decisive role in determining the sign and strength of the J values. Here we have developed magneto-structural correlation on complex **3** by varying the Gd–O distance and Gd–O–N angle. As the Gd–O distance increases, the J values tend to become less positive (see Fig. 5a). However, incorporation of the experimental points suggest a scattered pattern revealing that Gd–O distance is unlikely to be a unique parameter to influence the J values.

For the Gd–O–N angle, a parabolic behaviour was observed (Fig. 5b) where antiferromagnetic coupling was observed with larger Gd–O–N angles. The incorporation of the experimental point suggests a similar pattern although some of the experimental points deviate from the computed curve. To see if Gd–O and Gd–O–N angle parameters are correlated with each other, we have developed a three dimensional correlation by varying the Gd–O distances as well as the Gd–O–N angles simultaneously (see Fig. S10, ESI†). This correlation also reiterates the point that the Gd–O–N parameter is strongly influencing, especially for cases where magnetic behaviour switches from ferro to antiferromagnetic and this correlation is also not able to clearly predict the experimental trend.

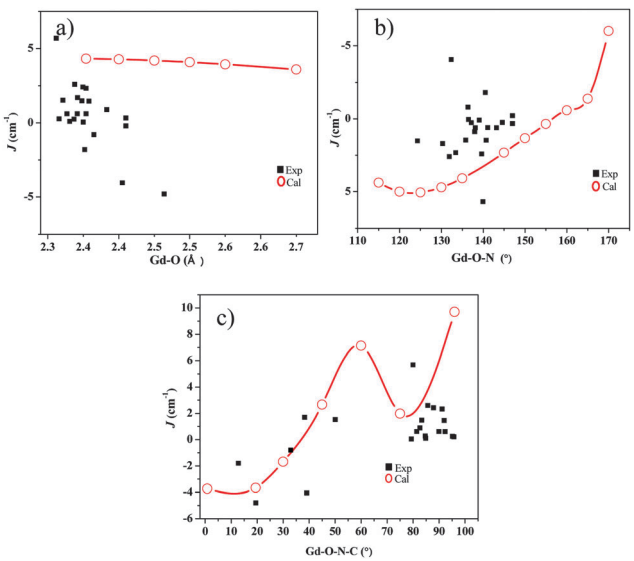

Fig. 5 Magneto-structural correlations developed by varying (a) Gd–O distance and (b) Gd–O–N angle in complex **3**, and (c) Gd–O–N–C dihedral angle in complex **9**. Black squares represent experimental points.

This journal is © the Owner Societies 2014

Published on 20 February 2014. Downloaded by INDIAN INSTITUTE OF TECHNOLOGY BOMBAY on 10/20/2020 12:24:49 PM.

Apart from the Gd–O bond distance and the Gd–O–N bond angle parameters, we also found a large variation in the Gd–O–N–C dihedral angle among the reported clusters (see Table 1). To understand the effect of this parameter, we have developed a correlation using complex **9** (see Fig. 5c) (note here that steric crowding of the ligands present in complex **3** does not allow for a large variation of dihedral angles). The dihedral angle correlation follows the experimental trend better compared with other parameters. As a whole, the developed magneto-structural correlations shows that no single parameter controls the nature of exchange interaction here, however both the bond angle and the dihedral angles effects are dominant in controlling the sign and nature of exchange interaction in this series.

4 Conclusions

Despite growing interest in {Gd^{III}–radical} complexes over the last decade, theoretical studies on these systems are still scarce. Here we have attempted to initiate this task by performing method assessment for the evaluation of magnetic exchange coupling constant. The conclusion derived from this work is summarised below.

(i) Incorporation of relativistic effects are found to be important for the Gd^{III} ions for the computation of J values. Although this can be done using ZORA or DKH methodology, relativistically corrected ECP basis sets are found to yield the lowest error compared to experimental observations.

(ii) The B2PLYP double-hybrid functional is found to yield very good numerical estimate of exchange coupling constant for all the ten complexes tested and this is followed very closely by the B3LYP functional. This suggests that addition of perturbative correlation energy improves the estimation of magnetic coupling in lanthanides and to the best of our knowledge, this is the first time a method assessment is being done for lanthanides using this new generation functional.

(iii) The mechanism of magnetic coupling established reveals a direct exchange between the 4f orbitals of Gd^{III} and the π^* magnetic orbital of the radical ligands. The MO and NBO analysis reveal that the empty orbitals of the Gd^{III} actively participate in the mechanism. Unlike in {Gd–3d} complexes where 5d orbitals exclusively are found to play a critical role, here all three 5d/6s/6p orbitals are found to play a role in mediating the exchange coupling.

(iv) Magneto-structural correlations suggest that changes in bond distance are negligible whereas the bond angle and the dihedral angle predict correctly the ferro-antiferro magnetic trend. An overlay of the experimental data on top of the developed correlation, however, suggests a scattered picture revealing the absence of unique structural parameters that control the nature of the exchange for the {Gd^{III}–2p} pair.

To this end, here for the first time we have attempted to perform a method assessment for reliable computation of magnetic exchange for {Gd^{III}–radical} pair and have established the generic mechanism of coupling. Since coupling constants are intricate parameters associated strongly with the distribution of unpaired spins, the outcome of this study has wider implications in the area of lanthanides, lanthanide–transition metals and lanthanide–radical chemistry.

Acknowledgements

GR would like to acknowledge the financial support from the Government of India through the Department of Science and Technology (SR/S1/IC-41/2010; SR/NM/NS-1119/2011) and generous computational resources from Indian Institute of Technology-Bombay. TG thanks UGC and TR thanks DST for a SRF fellowship.

References

1 R. Sessoli, D. Gatteschi, A. Caneschi and M. A. Novak, *Nature*, 1993, **365**, 141–143.
2 G. Christou, D. Gatteschi, D. N. Hendrickson and R. Sessoli, *MRS Bull.*, 2000, **25**, 66–71.
3 (*a*) M. N. Leuenberger and D. Loss, *Nature*, 2001, **410**, 789–793; (*b*) S. Hill, R. S. Edwards, N. Aliaga-Alcalde and G. Christou, *Science*, 2003, **302**, 1015–1018; (*c*) F. K. Larsen, E. J. L. McInnes, H. El Mkami, J. Overgaard, S. Piligkos, G. Rajaraman, E. Rentschler, A. A. Smith, G. M. Smith, V. Boote, M. Jennings, G. A. Timco and R. E. P. Winpenny, *Angew. Chem., Int. Ed.*, 2003, **42**, 101–105; (*d*) B. Fleury, L. Catala, V. Huc, C. David, W. Z. Zhong, P. Jegou, L. Baraton, S. Palacin, P. A. Albouy and T. Mallah, *Chem. Commun.*, 2005, 2020–2022; (*e*) M. Affronte, F. Troiani, A. Ghirri, A. Candini, M. Evangelisti, V. Corradini, S. Carretta, P. Santini, G. Amoretti, F. Tuna, G. Timco and R. E. P. Winpenny, *J. Phys. D: Appl. Phys.*, 2007, **40**, 2999–3004.
4 (*a*) L. Bogani and W. Wernsdorfer, *Nat. Mater.*, 2008, **7**, 179–186; (*b*) S. Sanvito, *Chem. Soc. Rev.*, 2011, **40**, 3336–3355.
5 (*a*) N. Ishikawa, M. Sugita, T. Ishikawa, S. Koshihara and Y. Kaizu, *J. Am. Chem. Soc.*, 2003, **125**, 8694–8695; (*b*) C. M. Zaleski, E. C. Depperman, J. W. Kampf, M. L. Kirk and V. L. Pecoraro, *Angew. Chem., Int. Ed.*, 2004, **43**, 3912–3914; (*c*) Y. Z. Zhang, W. Wernsdorfer, F. Pan, Z. M. Wang and S. Gao, *Chem. Commun.*, 2006, 3302–3304; (*d*) L. F. Chibotaru, L. Ungur and A. Soncini, *Angew. Chem., Int. Ed.*, 2008, **47**, 4126–4129; (*e*) C. E. Burrow, T. J. Burchell, P. H. Lin, F. Habib, W. Wernsdorfer, R. Clerac and M. Murugesu, *Inorg. Chem.*, 2009, **48**, 8051–8053; (*f*) Y. N. Guo, G. F. Xu, Y. Guo and J. K. Tang, *Dalton Trans.*, 2011, **40**, 9953–9963; (*g*) Y. N. Guo, G. F. Xu, Y. Guo and J. K. Tang, *Dalton Trans.*, 2011, **40**, 9953–9963; (*h*) B. Joarder, A. K. Chaudhari, G. Rogez and S. K. Ghosh, *Dalton Trans.*, 2012, **41**, 7695–7699; (*i*) S. Y. Lin, L. Zhao, H. S. Ke, Y. N. Guo, J. K. Tang, Y. Guo and J. M. Dou, *Dalton Trans.*, 2012, **41**, 3248–3252.
6 (*a*) M. Atanasov, B. Delley, F. Neese, P. L. Tregenna-Piggott and M. Sigrist, *Inorg. Chem.*, 2011, **50**, 2112–2124; (*b*) T. Jurca, A. Farghal, P. H. Lin, I. Korobkov, M. Murugesu and D. S. Richeson, *J. Am. Chem. Soc.*, 2011, **133**, 15814–15817.
7 S. K. Langley, K. J. Berry, B. Moubaraki and K. S. Murray, *Dalton Trans.*, 2009, 973–982.

Published on 20 February 2014. Downloaded by INDIAN INSTITUTE OF TECHNOLOGY BOMBAY on 10/20/2020 12:24:49 PM.

8 C. Boskovic, E. K. Brechin, W. E. Streib, K. Folting, J. C. Bollinger, D. N. Hendrickson and G. Christou, *J. Am. Chem. Soc.*, 2002, **124**, 3725–3736.
9 N. Ishikawa, M. Sugita and W. Wernsdorfer, *Angew. Chem., Int. Ed.*, 2005, **44**, 2931–2935.
10 (*a*) A. Caneschi, D. Gatteschi, R. Sessoli, A. L. Barra, L. C. Brunel and M. Guillot, *J. Am. Chem. Soc.*, 1991, **113**, 5873–5874; (*b*) D. Gatteschi, A. Caneschi, L. Pardi and R. Sessoli, *Science*, 1994, **265**, 1054–1058; (*c*) N. Roch, S. Florens, V. Bouchiat, W. Wernsdorfer and F. Balestro, *Nature*, 2008, **453**, 633–637.
11 (*a*) S. Takamatsu, T. Ishikawa, S. Y. Koshihara and N. Ishikawa, *Inorg. Chem.*, 2007, **46**, 7250–7252; (*b*) M. A. AlDamen, J. M. Clemente-Juan, E. Coronado, C. Marti-Gastaldo and A. Gaita-Arino, *J. Am. Chem. Soc.*, 2008, **130**, 8874–8875; (*c*) M. A. AlDamen, J. M. Clemente-Juan, E. Coronado, C. Marti-Gastaldo and A. Gaita-Arino, *J. Am. Chem. Soc.*, 2008, **130**, 8874–8875; (*d*) M. A. AlDamen, S. Cardona-Serra, J. M. Clemente-Juan, E. Coronado, A. Gaita-Arino, C. Marti-Gastaldo, F. Luis and O. Montero, *Inorg. Chem.*, 2009, **48**, 3467–3479; (*e*) D. Savard, P. H. Lin, T. J. Burchell, I. Korobkov, W. Wernsdorfer, R. Clerac and M. Murugesu, *Inorg. Chem.*, 2009, **48**, 11748–11754; (*f*) R. Sessoli and A. K. Powell, *Coord. Chem. Rev.*, 2009, **253**, 2328–2341; (*g*) Y. Y. Gao, Y. L. Wang, P. Hu, M. F. Yang, Y. Ma, Q. L. Wang, L. C. Li and D. Z. Liao, *Inorg. Chem. Commun.*, 2013, **27**, 31–35; (*h*) S. K. Langley, D. P. Wielechowski, V. Vieru, N. F. Chilton, B. Moubaraki, B. F. Abrahams, L. F. Chibotaru and K. S. Murray, *Angew. Chem., Int. Ed.*, 2013, **52**, 12014–12019; (*i*) M. Zhu, Y. G. Li, Y. Ma, L. C. Li and D. Z. Liao, *Inorg. Chem.*, 2013, **52**, 12326–12328.
12 (*a*) C. Aronica, G. Pilet, G. Chastanet, W. Wernsdorfer, J. F. Jacquot and D. Luneau, *Angew. Chem., Int. Ed.*, 2006, **45**, 4659–4662; (*b*) M. Ferbinteanu, T. Kajiwara, K. Y. Choi, H. Nojiri, A. Nakamoto, N. Kojima, F. Cimpoesu, Y. Fujimura, S. Takaishi and M. Yamashita, *J. Am. Chem. Soc.*, 2006, **128**, 9008–9009.
13 (*a*) V. M. Mereacre, A. M. Ako, R. Clerac, W. Wernsdorfer, G. Filoti, J. Bartolome, C. E. Anson and A. K. Powell, *J. Am. Chem. Soc.*, 2007, **129**, 9248–9249; (*b*) J. Cirera and E. Ruiz, *C. R. Chim.*, 2008, **11**, 1227–1234.
14 (*a*) J. P. Sutter, M. L. Kahn, S. Golhen, L. Ouahab and O. Kahn, *Chem.–Eur. J.*, 1998, **4**, 571–576; (*b*) A. Caneschi, A. Dei, D. Gatteschi, L. Sorace and K. Vostrikova, *Angew. Chem., Int. Ed.*, 2000, **39**, 246–248.
15 (*a*) A. Caneschi, A. Dei, D. Gatteschi, C. A. Massa, L. A. Pardi, S. Poussereau and L. Sorace, *Chem. Phys. Lett.*, 2003, **371**, 694–699; (*b*) D. Luneau and P. Rey, *Coord. Chem. Rev.*, 2005, **249**, 2591–2611; (*c*) G. Poneti, K. Bernot, L. Bogani, A. Caneschi, R. Sessoli, W. Wernsdorfer and D. Gatteschi, *Chem. Commun.*, 2007, 1807–1809.
16 E. Ruiz, A. Rodriguez-Fortea, J. Cano, S. Alvarez and P. Alemany, *J. Comput. Chem.*, 2003, **24**, 982–989.
17 G. Rajaraman, F. Totti, A. Bencini, A. Caneschi, R. Sessoli and D. Gatteschi, *Dalton Trans.*, 2009, 3153–3161.
18 T. Rajeshkumar, S. K. Singh and G. Rajaraman, *Polyhedron*, 2013, **52**, 1299–1305.
19 C. Lescop, E. Belorizky, D. Luneau and P. Rey, *Inorg. Chem.*, 2002, **41**, 3375–3384.
20 Y. L. Wang, Y. Y. Gao, Y. Ma, Q. L. Wang, L. C. Li and D. Z. Liao, *J. Solid State Chem.*, 2013, **202**, 276–281.
21 J. X. Xu, Y. Ma, G. F. Xu, C. Wang, D. Z. Liao, Z. H. Jiang, S. P. Yan and L. C. Li, *Inorg. Chem. Commun.*, 2008, **11**, 1356–1358.
22 C. Wang, Y. L. Wang, Z. X. Qin, Y. Ma, Q. L. Wang, L. C. Li and D. Z. Liao, *Inorg. Chem. Commun.*, 2012, **20**, 112–116.
23 C. Lescop, D. Luneau, P. Rey, G. Bussiere and C. Reber, *Inorg. Chem.*, 2002, **41**, 5566–5574.
24 C. Benelli, A. Caneschi, D. Gatteschi and L. Pardi, *Inorg. Chem.*, 1992, **31**, 741–746.
25 Q. H. Zhao, Y. P. Ma, L. Du and R. B. Fang, *Transition Met. Chem.*, 2006, **31**, 593–597.
26 C. X. Zhang, N. N. Sun, X. Y. Zhao, Y. Y. Zhang and Y. L. Guo, *Inorg. Chem. Commun.*, 2011, **14**, 166–168.
27 N. Zhou, Y. Ma, C. Wang, G. F. Xu, J. K. Tang, S. P. Yan and D. Z. Liao, *J. Solid State Chem.*, 2010, **183**, 927–932.
28 Y. Q. Qi, Z. H. Jiang, D. Z. Liao and G. L. Wang, *Synth. React. Inorg. Met.–Org. Chem.*, 1997, **27**, 347–359.
29 C. Benelli, A. Caneschi, D. Gatteschi, J. Laugier and P. Rey, *Angew. Chem., Int. Ed. Engl.*, 1987, **26**, 913–915.
30 C. Benelli, A. Caneschi, D. Gatteschi, L. Pardi and P. Rey, *Inorg. Chem.*, 1990, **29**, 4223–4228.
31 C. Benelli, A. Caneschi, D. Gatteschi, L. Pardi and P. Rey, *Inorg. Chem.*, 1989, **28**, 275–280.
32 X. L. Wang, *Inorg. Chim. Acta*, 2012, **387**, 20–24.
33 X. L. Wang, P. P. Xu, X. Bao, F. W. Wang, Y. H. Chen and Y. J. Wei, *Z. Anorg. Allg. Chem.*, 2013, **639**, 176–180.
34 T. Tsukuda, T. Suzuki and S. Kaizaki, *Inorg. Chim. Acta*, 2005, **358**, 1253–1257.
35 T. Tsukuda, T. Suzuki and S. Kaizaki, *J. Chem. Soc., Dalton Trans.*, 2002, 1721–1726.
36 T. Ishida, R. Murakami, T. Kanetomo and H. Nojiri, *Polyhedron*, 2013, **66**, 183–187.
37 J. D. Rinehart, M. Fang, W. J. Evans and J. R. Long, *Nat. Chem.*, 2011, **3**, 538–542.
38 X. W. Peng Hu, Y. Ma, Q. Wang, L. Li and D. Liao, *Dalton Trans.*, 2014, **43**, 2234–2243.
39 F. Pointillart, Y. Le Gal, S. Golhen, O. Cador and L. Ouahab, *Chem. Commun.*, 2009, 3777–3779.
40 L. Noodleman, *J. Chem. Phys.*, 1981, **74**, 5737–5743.
41 S. K. Singh, N. K. Tibrewal and G. Rajaraman, *Dalton Trans.*, 2011, **40**, 10897–10906.
42 (*a*) E. Ruiz, J. Cano, S. Alvarez and P. Alemany, *J. Comput. Chem.*, 1999, **20**, 1391–1400; (*b*) E. Ruiz, J. Cano, S. Alvarez, A. Caneschi and D. Gatteschi, *J. Am. Chem. Soc.*, 2003, **125**, 6791–6794; (*c*) P. Christian, G. Rajaraman, A. Harrison, M. Helliwell, J. J. W. McDouall, J. Raftery and R. E. P. Winpenny, *Dalton Trans.*, 2004, 2550–2555; (*d*) G. Rajaraman, J. Cano, E. K. Brechin and E. J. L. McInnes, *Chem. Commun.*, 2004, 1476–1477; (*e*) S. Piligkos, G. Rajaraman, M. Soler, N. Kirchner, J. van Slageren, R. Bircher, S. Parsons, H. U. Gudel, J. Kortus,

 This journal is © the Owner Societies 2014

Published on 20 February 2014. Downloaded by INDIAN INSTITUTE OF TECHNOLOGY BOMBAY on 10/20/2020 12:24:49 PM.

W. Wernsdorfer, G. Christou and E. K. Brechin, *J. Am. Chem. Soc.*, 2005, **127**, 5572–5580.

43 (*a*) K. Hegetschweiler, B. Morgenstern, J. Zubieta, P. J. Hagrman, N. Lima, R. Sessoli and F. Totti, *Angew. Chem., Int. Ed.*, 2004, **43**, 3436–3439; (*b*) G. Rajaraman, M. Murugesu, E. C. Sanudo, M. Soler, W. Wernsdorfer, M. Helliwell, C. Muryn, J. Raftery, S. J. Teat, G. Christou and E. K. Brechin, *J. Am. Chem. Soc.*, 2004, **126**, 15445–15457; (*c*) A. Bencini and F. Totti, *Int. J. Quantum Chem.*, 2005, **101**, 819–825.

44 M. Frisch, G. W. Trucks, H. B. Schlegel, G. E. Scuseria, M. A. Robb, J. R. Cheeseman, G. Scalmani, V. Barone, B. Mennucci, G. A. Petersson, H. Nakatsuji, M. Caricato, X. Li, H. P. Hratchian, A. F. Izmaylov, J. Bloino, G. Zheng, J. L. Sonnenberg, M. Hada, M. Ehara, K. Toyota, R. Fukuda, J. Hasegawa, M. Ishida, T. Nakajima, Y. Honda, O. Kitao, H. Nakai, T. Vreven, J. A. Montgomery Jr, J. E. Peralta, F. Ogliaro, M. Bearpark, J. J. Heyd, E. Brothers, K. N. Kudin, V. N. Staroverov, R. Kobayashi, J. Normand, K. Raghavachari, A. Rendell, J. C. Burant, S. S. Iyengar, J. Tomasi, M. Cossi, N. Rega, J. M. Millam, M. Klene, J. E. Knox, J. B. Cross, V. Bakken, C. Adamo, J. Jaramillo, R. Gomperts, R. E. Stratmann, O. Yazyev, A. J. Austin, R. Cammi, C. Pomelli, J. W. Ochterski, R. L. Martin, K. Morokuma, V. G. Zakrzewski, G. A. Voth, P. Salvador, J. J. Dannenberg, S. Dapprich, A. D. Daniels, Ö. Farkas, J. B. Foresman, J. V. Ortiz, J. Cioslowski and D. J. Fox, *Gaussian 09, Rev. D, 01*, Gaussian, Inc., Wallingford CT, 2009.

45 T. R. Cundari and W. J. Stevens, *J. Chem. Phys.*, 1993, **98**, 5555–5565.

46 A. Schafer, C. Huber and R. Ahlrichs, *J. Chem. Phys.*, 1994, **100**, 5829–5835.

47 D. A. Pantazis and F. Neese, *J. Chem. Theory Comput.*, 2009, **5**, 2229–2238.

48 B. A. Hess, *Phys. Rev. A: At., Mol., Opt. Phys.*, 1985, **32**, 756–763.

49 (*a*) M. Douglas and N. M. Kroll, *Ann. Phys.*, 1974, **82**, 89–155; (*b*) E. Vanlenthe, E. J. Baerends and J. G. Snijders, *J. Chem. Phys.*, 1993, **99**, 4597–4610.

50 F. Neese, *Orca*, Bonn, 2010.

51 T. Rajeshkumar and G. Rajaraman, *Chem. Commun.*, 2012, **48**, 7856–7858.

52 (*a*) J. P. Perdew, *Phys. Rev. B: Condens. Matter Mater. Phys.*, 1986, **33**, 8822–8824; (*b*) A. D. Becke, *Phys. Rev. A: At., Mol., Opt. Phys.*, 1988, **38**, 3098–3100.

53 (*a*) J. P. Perdew and Y. Wang, *Phys. Rev. B: Condens. Matter Mater. Phys.*, 1992, **45**, 13244–13249; (*b*) J. P. Perdew, K. Burke and M. Ernzerhof, *Phys. Rev. Lett.*, 1996, **77**, 3865–3868.

54 C. T. Lee, W. T. Yang and R. G. Parr, *Phys. Rev. B: Condens. Matter Mater. Phys.*, 1988, **37**, 785–789.

55 N. C. Handy and A. J. Cohen, *Mol. Phys.*, 2001, **99**, 403–412.

56 (*a*) J. P. Perdew, in *Electronic Structure of Solids*, ed. P. Ziesche and H. Eschrig, Akademie Verlag, Berlin, 1991, pp. 11–20; (*b*) J. P. P. K. Burke and Y. Wang, in *Electronic Density Functional Theory: Recent Progress and New Directions*, ed. J. F. Dobson, G. Vignale and M. P. Das, Plenum, 1998; (*c*) J. P. Perdew, J. A. Chevary, S. H. Vosko, K. A. Jackson, M. R. Pederson, D. J. Singh and C. Fiolhais, *Phys. Rev. B: Condens. Matter Mater. Phys.*, 1992, **46**, 6671–6687; (*d*) J. P. Perdew, J. A. Chevary, S. H. Vosko, K. A. Jackson, M. R. Pederson, D. J. Singh and C. Fiolhais, *Phys. Rev. B: Condens. Matter Mater. Phys.*, 1993, **48**, 4978; (*e*) J. P. Perdew, K. Burke and Y. Wang, *Phys. Rev. B: Condens. Matter Mater. Phys.*, 1996, **54**, 16533–16539.

57 (*a*) J. P. Perdew, M. Emzerhof and K. Burke, *J. Chem. Phys.*, 1996, **105**, 9982–9985; (*b*) C. Adamo and V. Barone, *J. Chem. Phys.*, 1999, **110**, 6158–6170; (*c*) M. Ernzerhof and G. E. Scuseria, *J. Chem. Phys.*, 1999, **110**, 5029–5036.

58 (*a*) A. D. Becke, *J. Chem. Phys.*, 1993, **98**, 5648–5652; (*b*) P. J. Stephens, F. J. Devlin, C. F. Chabalowski and M. J. Frisch, *J. Phys. Chem.*, 1994, **98**, 11623–11627.

59 (*a*) V. N. Staroverov, G. E. Scuseria, J. M. Tao and J. P. Perdew, *J. Chem. Phys.*, 2003, **119**, 12129–12137; (*b*) J. M. Tao, J. P. Perdew, V. N. Staroverov and G. E. Scuseria, *Phys. Rev. Lett.*, 2003, **91**, 146401–146404.

60 S. Grimme, *J. Chem. Phys.*, 2006, **124**, 034108–034116.

61 M. J. T. Frisch, G. W. Trucks, H. B. Schlegel, P. M. W. Gill, B. G. Johnson, M. W. Wong, J. B. Foresman, M. A. Robb, M. Head-Gordon, E. S. Replogle, R. Gomperts, J. L. Andres, K. Raghavachari, J. S. Binkley, C. Gonzalez, R. L. Martin, D. J. Fox, D. J. Defrees, J. Baker, J. J. P. Stewart and J. A. Pople, *GAUSSIAN 92/DFT, Revision F.4*, Gaussian, Pittsburgh, 1993.

62 (*a*) J. Paier, M. Marsman, K. Hummer, G. Kresse, I. C. Gerber and J. G. Angyan, *J. Chem. Phys.*, 2006, **125**, 154709; (*b*) J. L. F. Da Silva, M. V. Ganduglia-Pirovano, J. Sauer, V. Bayer and G. Kresse, *Phys. Rev. B: Condens. Matter Mater. Phys.*, 2007, **75**, 045121; (*c*) M. De La Pierre, R. Orlando, L. Maschio, K. Doll, P. Ugliengo and R. Dovesi, *J. Comput. Chem.*, 2011, **32**, 1775–1784.

63 F. Neese, T. Schwabe, S. Kossmann, B. Schirmer and S. Grimme, *J. Chem. Theory Comput.*, 2009, **5**, 3060–3073.

64 T. Schwabe and S. Grimme, *J. Phys. Chem. Lett.*, 2010, **1**, 1201–1204.

65 E. Cremades, S. Gomez-Coca, D. Aravena, S. Alvarez and E. Ruiz, *J. Am. Chem. Soc.*, 2012, **134**, 10532–10542.